의학석사 학위논문

Optimum tension for the bridging sutures in trans-osseous equivalent rotator cuff repair
- Cadaveric biomechanical study –

관절경적 회전근 개 교량형 봉합술시 봉합사에 가해지는 적절한 장력에 대한 사체 생 역학 연구

2014 년 8 월

서울대학교 대학원

의학과 정형외과학 전공

박 지 순

A thesis of the Master's degree

Optimum tension for the bridging sutures in trans-osseous equivalent rotator cuff repair
- Cadaveric biomechanical study -

관절경적 회전근 개 교량형 봉합술시 봉합사에 가해지는 적절한 장력에 대한 사체 생 역학 연구

August 2014

The Department of Orthopedic Surgery,

Seoul National University

College of Medicine

Ji Soon Park

관절경적 회전근 개 교량형 봉합술시 봉합사에 가해지는 적절한 장력에 대한 사체 생 역학 연구

지도교수 오 주 한

이 논문을 의학 석사 학위논문으로 제출함

2014년 7월

서울대학교 대학원

의학과 정형외과학 전공

박 지 순

박 지 순의 의학 석사 학위논문을 인준함

2014년 7월

위 원 장 최 정 아 (인)

부 위 원 장 오 주 한 (인)

위 원 김 세 훈 (인)

Abstract

Background: Transosseous-equivalent (TOE) rotator cuff repair can increase contact area and contact pressure between the repaired cuff tendon and bony footprint and show higher ultimate load to failure and smaller gap formation compared with other repair techniques. However, it has been suggested that medial rotator cuff failure after TOE repair may result from increased bridging suture tension.

Purpose: To determine optimum bridging suture tension in TOE repair by evaluating footprint contact and construct failure characteristics at different tensions.

Study Design: Controlled laboratory study.

Methods: Eighteen fresh-frozen cadaveric shoulders, randomly divided into 3 groups, were constructed with TOE configuration using the same medial suture

anchor, placing a Tekscan sensing pad between repaired cuff tendon and footprint. Nine of the 18 shoulders were used to measure footprint-contact characteristics. Using the Tekscan measurement system, contact pressure between the rotator cuff tendon and greater tuberosity was quantified for bridging suture tensions of 60, 90, and 120 N at glenohumeral abduction angles of 0° and 30° and humeral rotation angles of −30°, 0°, and +30°. TOE constructs of all 18 shoulders then underwent cyclic-loading and load-to-failure tests. Yield load, ultimate load, stiffness, hysteresis, strain, and failure mode in construct-failure tests (cyclic-loading and load-to-failure tests) were evaluated in 3 groups: 2 Versalok tension groups (60 and 120 N) and a maximum tension of other type lateral anchor group.

Results: As bridging suture tension increased, contact force, contact pressure, and peak pressure increased significantly at all positions (all $P < .05$). However, regarding contact area, no significant differences were found between 90 and 120 N at all positions, although there were significant differences between 60 and 90 N. From the construct failure test, there were no significant differences

in any parameters according to various tensions or anchor types (all $P > .05$).

Conclusion: Increasing bridging suture tension over 90 N did not improve contact area but did increase contact force and pressure. Bridging suture tension did not significantly affect ultimate failure loads.

Clinical Relevance: Considering risks for over-tensioning of bridging sutures, it might be clinically more relevant to not set the bridging suture tension over 90 N.

KeyWords: Rotator cuff repair, Transosseous-equivalent, bridging suture tension

Student number : 2012-23615

목 차

표 및 그림 목록

Introduction

Rotator cuff tear is one of the most common and important shoulder conditions encountered by orthopedic surgeons (1-3). Furthermore, the prevalence of rotator cuff tear is increasing rapidly with the aging population and the popularity of sports activities with older people (4, 5).

In general, it is well accepted that conservative treatment cannot heal the rotator cuff tear itself. A rotator cuff tear tends to progress with time in terms of tear size and symptoms, and a larger tear size and advanced fatty infiltration of rotator cuff muscles are associated with healing failure after surgical repair. These factors can be possible reasons for early surgical intervention and the steep increase in the volume of rotator cuff repairs (2, 6-10).

A number of inherent factors affect clinical outcomes after rotator cuff repair, including tear size, muscle atrophy, fatty infiltration of rotator cuff muscles, chronicity of symptoms, and osteoporosis (8-12). These factors cannot be controlled by surgeons. However, the types of surgical implants, instruments, repair techniques, and repair constructs are modifiable factors that can be changed by the surgeons. Among these modifiable factors, more attention is

focused on the concept of anatomic restoration of the rotator cuff on the footprint. Stable fixation of rotator cuff and biomechanical properties of the tendon-bone surface area may be more critical to achieve rotator cuff healing (13, 14). To achieve mechanical stability of the rotator cuff repair construct, numerous repair techniques have been developed and are currently used. Compared with many repair techniques, the modified double-row (transosseous-equivalent [TOE]) repair technique has increased contact surface area and mean contact pressure between the repaired cuff tendon and bony footprint and shows higher ultimate load to failure and smaller gap formation (12, 15).

There is an opinion that increased bridging suture tension can increase contact pressure and contact area between the repaired tendon and footprint, consequently enhancing cuff healing, as shown in animal model and cadaveric studies (13, 16,17). However, results of these time-zero studies cannot always be applied to the clinical situation.

Moreover, recent articles have reported medial rotator cuff failure after double-row and suture bridge repair (18-21), listing potential risk factors for

this new type of failure as tension overload at the medial row, several problems caused by retrograde suture passage, and the effect of the braided suture materials. In another study, the TOE repair technique reduces intratendinous blood supply at the tendon repair site (22). Therefore, too much bridging suture tension can be a risk factor of medial rotator cuff failure by compromising blood flow of the compressed tendon in TOE rotator cuff repair. It is important to acknowledge that a certain degree of bridging suture tension is optimal for rotator cuff tendon healing in the clinical situation.

The main purpose of the current study was to verify the relationship between bridging suture tension and contact pressure and thereby to find the optimum tension of the bridging sutures in TOE rotator cuff repair using Versalok® (Depuy Mitek, Raynham, MA) in a cadaveric model. In addition, we examined these contact characteristics with other type of lateral anchor (ReelX® ; Stryker Endoscopy, San Jose, CA) to verify whether these data can be used as reference. Another purpose of our study was to measure the load to failure of the repaired construct according to various bridging suture tensions to identify whether bridging suture tension affects the stability of the repaired construct.

MATERIALS AND METHODS

Tensiometer

We used a custom-made tensiometer (Figure 1), attachable to the Versalok® system, to measure the bridging suture tension in both cadaveric and clinical studies.

Figure 1. Tensiometer with Versalok® is shown.

Preliminary Data

Due to the absence of previous data on bridging suture tension of Versalok®, we designed preliminary experiments to determine the maximum bridging suture tension of Versalok® from rotator cuff repairs performed in the senior author's institution and then decided to test 3 tensions: 50%, 75%, and 100% of the maximum tension.

To find the usual maximum bridging suture tension applied with Versalok®, we used our custom-made tensiometer with Versalok® intraoperatively in 13 patients undergoing rotator cuff repairs (23). Maximum tension was measured by a senior surgeon, and the mean maximum tension was 115.56 N (79.98–159.96 N, median 99.98 N). Therefore, we determined mean maximum tension of Versalok® to be 120 N. Finally, we decided to test 60, 90, and 120 N as 50%, 75%, and 100% of the maximum tension, respectively, in the footprint-contact characteristics measurement. For the construct-failure test, we decided to test 60 and 120 N of Versalok® and the maximum tension of ReelX® because we judged that the interval of 30 N would not make a significant difference in load to failure.

Sample Size

The sample size calculation was performed with $\alpha = 0.05$ and power = 0.80. To detect an average contact pressure difference of a minimum 2 standard deviations among the 3 tension groups required a sample size of 6 in each group. The mean and standard deviation of contact pressure (0.27 ± 0.04 MPa) were based on the data of Park et al (12). The load-to-failure test of the repaired construct also required 6 in each group according to the data of Park et al (24). Because we could measure the footprint-contact characteristics repeatedly in the same cadaveric shoulder, the number of shoulders required was determined by the construct-failure test.

Specimen Preparation

Eighteen fresh-frozen human cadaveric shoulders (mean age, 58.3 ± 10.9 years; range, 31–65 years) without gross evidence of rotator cuff injury or humeral head defects were used for the biomechanical tests. Eleven specimens were obtained from male cadavers. The cadaveric specimens were stored at −20℃ until the day before testing and thawed for 24 hours at room temperature

before preparation for dissection and testing. All soft tissues were dissected from the scapula and proximal humerus. The humerus was cut transversely at the shaft 9 cm distal from the surgical neck. The shaft region was then potted with plaster of Paris in a polyvinyl chloride (PVC) pipe and fixed with a screw to be easily attached to our custom-made testing machines. The proximal humerus footprint was prepared with a rasp to expose a clear bony surface similar to actual surgery. After the supraspinatus tendon was removed from its humeral insertion, the distal 10 mm of tendon was removed to simulate a chronic rotator cuff tear (12, 15, 24). The specimens were kept moistened with a physiological saline solution to prevent dehydration during preparation and testing.

Pressure-Sensing Methods

Contact force, pressure, and area between repaired cuff tendon and footprint were measured with the Tekscan® system (Tekscan Inc., South Boston, MA). The sensor was customized as 8 mm (medial to lateral) by 2 cm (anterior to posterior) to maximize footprint coverage and sealed with clear waterproof tape.

After calibration with an Instron® load cell (Instron Corp, Canton, MA), the Tekscan® sensing pad was fixed using one anterior and one posterior small screw on the footprint (Figure 2). Throughout the pilot study, the sealing method did not affect the sensitivity and repeatability of the Tekscan® sensing pad, and the customized size of 160 mm^2 was considered suitable for covering a sufficient footprint area (24).

Figure 2. Tekscan® sensing pad was sealed with waterproof tape and fixed on the footprint of the greater tuberosity with two screws.

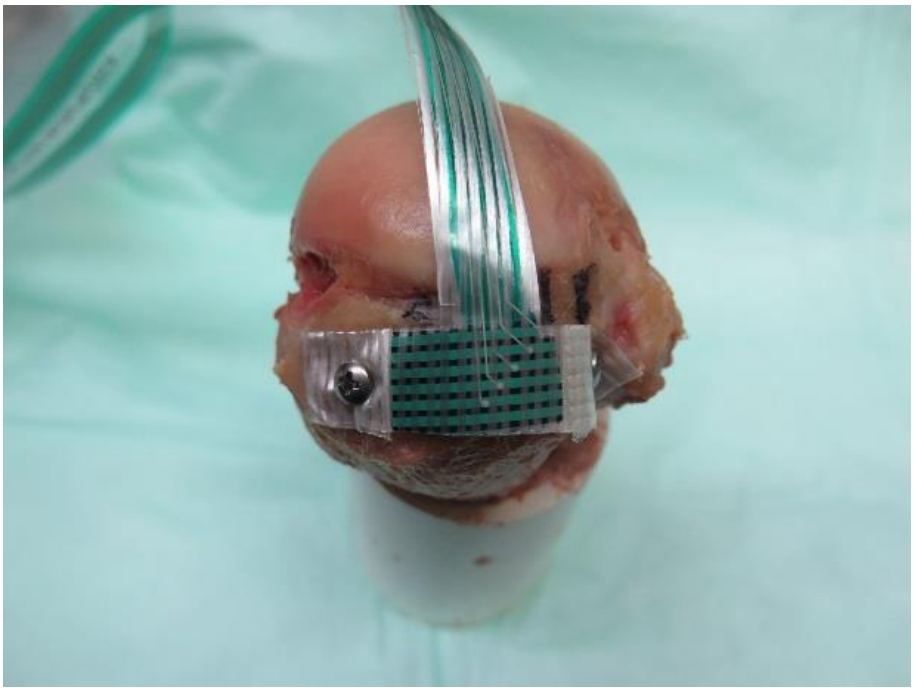

Repair Techniques

All cadaveric shoulders were constructed with a TOE configuration using the same double-loaded medial suture anchor (HEALIX® ; Depuy Mitek, Raynham, MA) and with a Tekscan® sensing pad placed between the repaired cuff tendon and footprint. The medial anchors were placed just lateral to the articular cartilage, with the anterior one located 5 mm posterior to the bicipital groove and the posterior one located 12.5 mm posterior to the anteromedial anchor. All medial anchors were inserted at a 45° angle relative to the footprint surface. After all the suture ends were passed through just lateral to the musculotendinous junction of the supraspinatus tendon, ties were made with a single sliding knot (SMC knot) augmented by 3 alternative half-hitch knots. A single surgeon performed all the repairs.

For Footprint Contact Characteristics Measurement.

After making 4 medial row ties using a horizontal mattress configuration, 2 metal anchors that had suture-passing holes (Corkscrew® ; Arthrex, Naples, FL) were inserted 2 cm distal to the footprint margin. Each metal anchor was in line

with the medial anchors positioned 12.5 mm apart in the anterior-posterior direction. Sutures from the first and third ties were then passed through the hole of the anterior metal anchor, and sutures from the second and fourth ties were passed through the hole of the posterior metal anchor. Finally, a rod was inserted firmly at the humerus shaft area for the attachment of our tensiometer (Figure 3)

For Construct Failure Test.

After footprint contact characteristics measurement, sutures in the metal anchor holes were retrieved, and the metal anchors and inserted rod were removed from the humerus. Sutures from the first and third ties were then pulled laterally and anchored 1 cm from the lateral margin of the footprint by the anterolateral anchor. Tension was determined using the tensiometer according to groups (60 N of Versalok®, 120 N of Versalok® and maximum tension of ReelX®). Sutures from the second and fourth ties were anchored by the posterolateral anchor by the same method. All of the lateral anchors were in line with the medial anchors positioned 12.5 mm apart in the anterior-posterior direction (12, 17, 24, 25).

Figure 3. Suture bridge repair configuration (left) and construct for tension-pressure measurement (right) are shown.

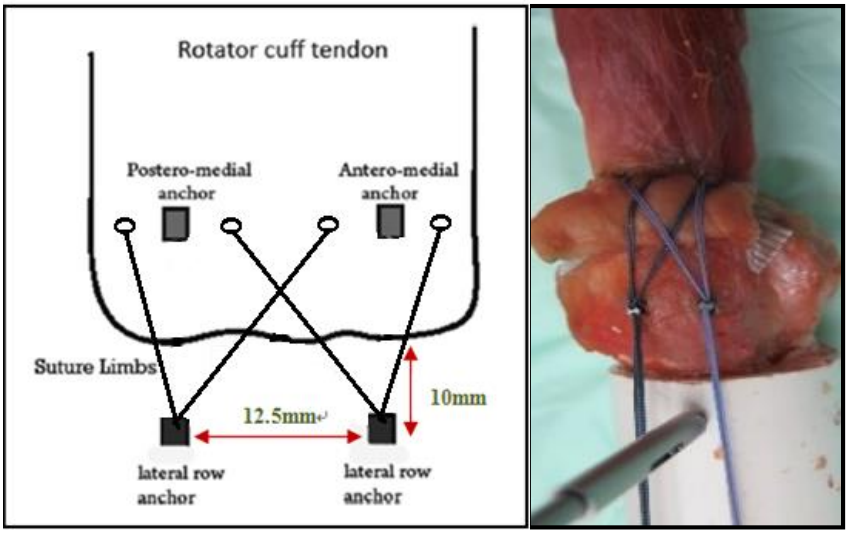

Biomechanical Testing

Footprint Contact Characteristics Measurement.

The prepared construct was fixed to the custom-made testing machine designed to change the abduction angle and rotation of the humeral head. Using the Tekscan® measurement system, contact force, peak pressure, mean pressure, and contact area between the rotator cuff tendon and the footprint were quantified for bridging suture tensions of 60, 90, and 120 N at glenohumeral abduction angles of 0° and 30° and humeral rotation angles of −30°, 0°, and +30° (Figure 4). The abduction angle was measured with an electronic goniometer, and neutral rotation was defined using the direction of the supraspinatus load vector. In total, 18 measurements were performed on each shoulder (2 abduction angles × 3 rotation angles × 3 tensions). To avoid the effects of the previous measurements and the stress-relaxation phenomenon, we did not make a final construct during footprint contact characteristics measurement. Instead, we exerted the designated tension manually each time after humeral head positioning, and tension was reduced to 0 after every measurement, which was confirmed with the Tekscan® sensor output (Figure

5). The inserted tension started at 60 N and was increased serially to 120 N. For each measurement, an interlocking whip stitch using No. 2 suture was made at the supraspinatus muscle belly, and the other end of the suture was passed to the pulley. A 30 N load was then applied and maintained during measurements that simulated a physiological load applied to the repaired supraspinatus tendon (14, 24-26).

Additionally, 3 cadaveric shoulders were used to measure the ReelX® contact characteristics for estimating the ReelX® tension based on the Versalok® data.

Construct failure test.

After footprint contact characteristics measurement, the TOE constructs of all 18 cadaveric shoulders were subjected to cyclic-loading and load-to-failure tests using an Instron® materials testing machine (model 3365) with a load cell capacity of 5 kN and a video digitizing system (VDS®; WINAnalyze; Micromark, Berlin, Germany). The 18 constructs were randomly divided into two Versalok® tension groups (60 and 120 N) and a maximum ReelX® tension group.

Each humerus was fixed at the shaft with the long axis of the humerus shaft placed at approximately 135° to the load actuator such that the traction axis was similar to actual postoperative states (27-29), and the supraspinatus muscle belly was placed in a custom-made freezing clamp and frozen in situ with liquid nitrogen. The liquid nitrogen was added until the freezing front was reached 2–3 mm medial to the medial suture ties. Once the fixation was finalized, 9 markers were placed on the surface of the tendon, bony surface of the humeral head, and clamp for VDS® analysis (Figure 6).

For the cyclic-loading test, constructs were preloaded with 10 N for 60 seconds and then cycled from 10 to 180 N at a loading rate of 1 mm/s for 30 cycles. During the cyclic loading, anterior and posterior gap formation, anterior and posterior footprint strain, anterior and posterior musculotendinous junction strain, hysteresis, and initial and linear stiffness were recorded for cycles 1 and 30 (15, 25, 29).

After the cyclic loading for 30 cycles, the load-to-failure test was performed. A 10 N preload was reapplied for 60 seconds, and then specimens were loaded at a rate of 1 mm/s until construct failure occurred. The yield load, ultimate load,

absorbed energy, displacement at yield load, and ultimate load were measured and calculated (15, 25).

Figure 4. Prepared construct was fixed to the custom-made testing machine designed to change abduction angle and humeral head rotation. The tensiometer was attached to the construct to apply the determined tension.

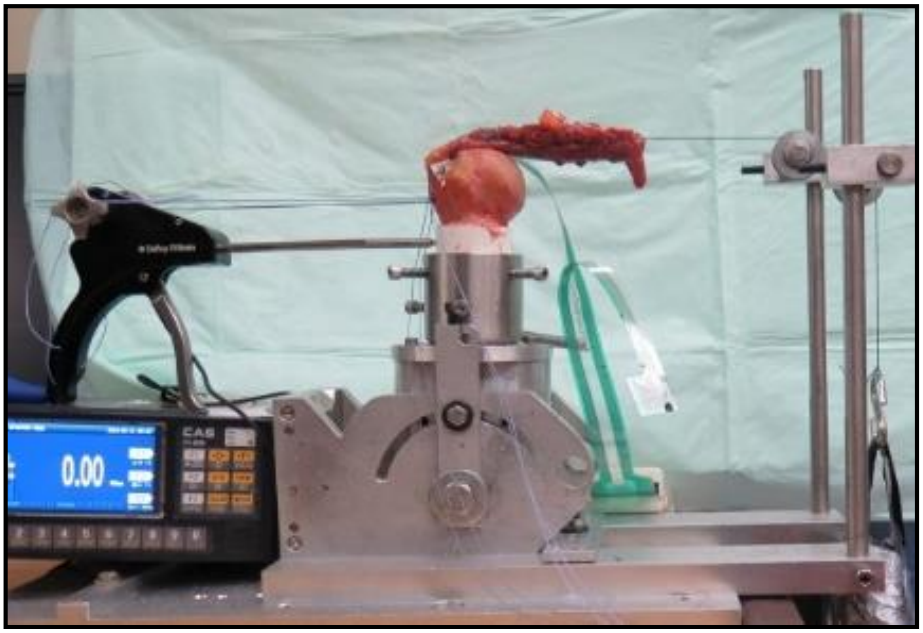

Figure 5. Example of tension-pressure raw data using the Tekscan® system is shown. The blue areas indicate contact surface, and red indicates higher-pressure areas.

N, neutral rotation, ER, external rotation 30°, IR, internal rotation 30°.

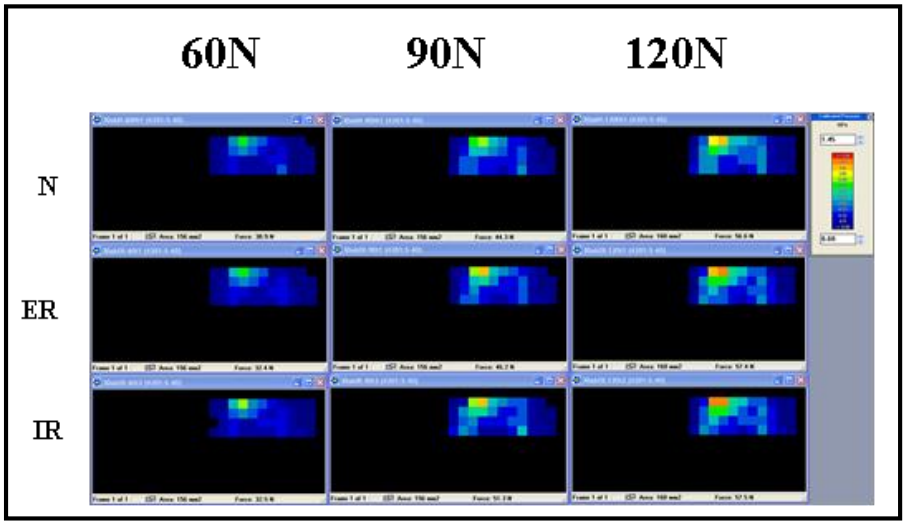

Figure 6. The construct was fixed to the Instron® testing machine, and the supraspinatus muscle belly was clamped and frozen with liquid nitrogen (left). Markers for the video digitizing system are shown on the right.

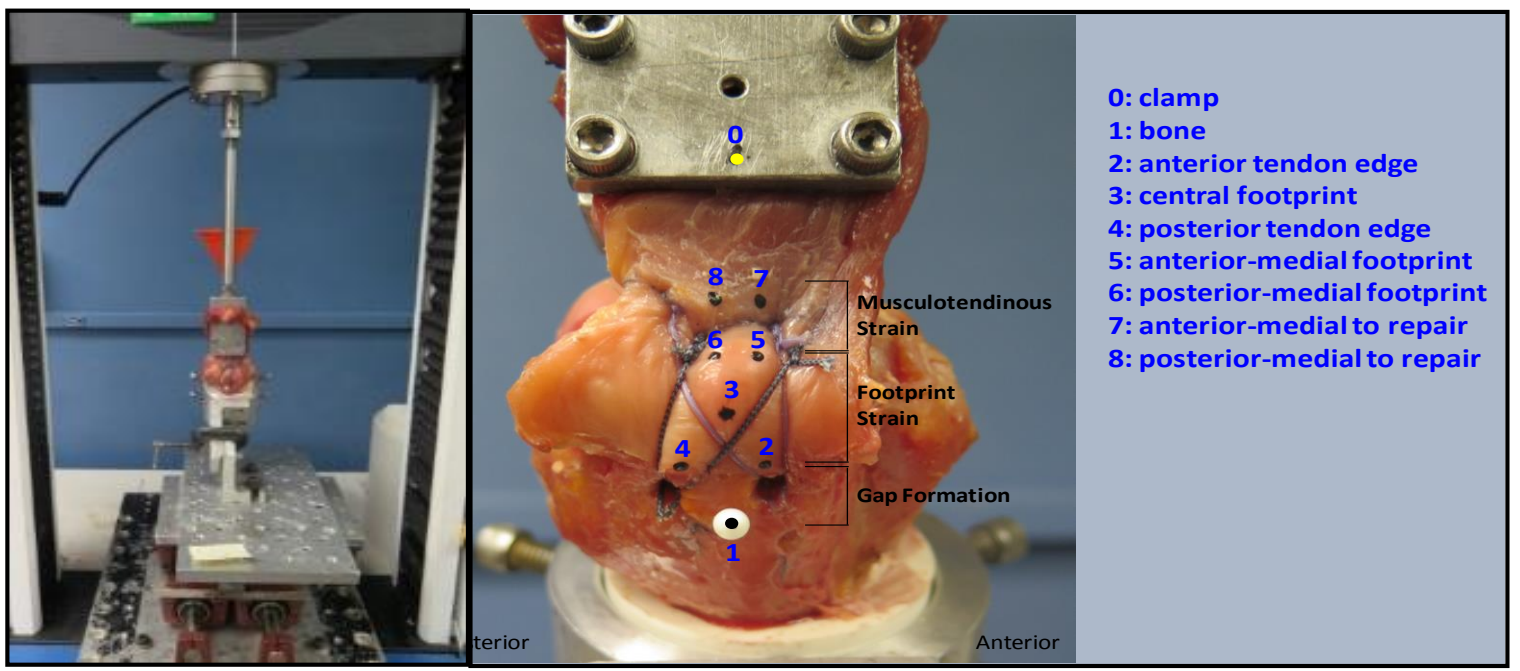

Statistical Analysis

Repeated-measures ANOVA was used to compare contact characteristics for the 3 different tensions under each circumstance. Linear regression was used to estimate the ReelX® tension based on the Versalok® data. One-way ANOVA was used to compare the variables in the construct-failure test for 60 and 120 N of Versalok® and the maximum tension of ReelX®.

RESULTS

Footprint Contact Characteristics Measurement

As the bridging suture tension was increased from 60 to 120 N, contact force, peak pressure, and mean pressure increased significantly at all positions (all $P < .05$; Table 1 and Figure 7). However, regarding the contact area, even though there were significant differences between 60 and 90 N except for 1 position (30° abduction and 30° external rotation), no significant differences were observed between 90 and 120 N at all positions (all $P > .05$; Table 2 and Figure 8). The maximum bridging suture tension for ReelX® estimated using the footprint-contact characteristics of Versalok® data was 157.8 ± 8.86 N.

TABLE 1

Contact Pressure Comparisons for Bridging Suture Tension According to Various Abduction Angles and Humeral Rotations[a]

Tension, N	Contact Pressure, MPa					
	Abduction 0°			Abduction 30°		
	Rotation −30°[b]	Rotation 0°	Rotation +30°	Rotation −30°[b]	Rotation 0°	Rotation +30°
60	0.17 ± 0.01	0.15 ± 0.01	0.18 ± 0.01	0.18 ± 0.01	0.16 ± 0.01	0.17 ± 0.00
90	0.24 ± 0.01	0.22 ± 0.01	0.25 ± 0.01	0.25 ± 0.01	0.23 ± 0.01	0.24 ± 0.00
120	0.30 ± 0.01	0.28 ± 0.01	0.31 ± 0.01	0.32 ± 0.01	0.30 ± 0.01	0.30± 0.01

[a]As tension was increased, pressure between the repaired tendon and footprint significantly increased.

Differences were statistically significant between all groups at all positions.

[b]The negative angle indicates means internal rotation.

Figure 7. Footprint contact characteristics measurement is shown. As tension was increased, pressure between the repaired cuff tendon and footprint increased significantly. Differences between all groups at all positions were statistically significant.

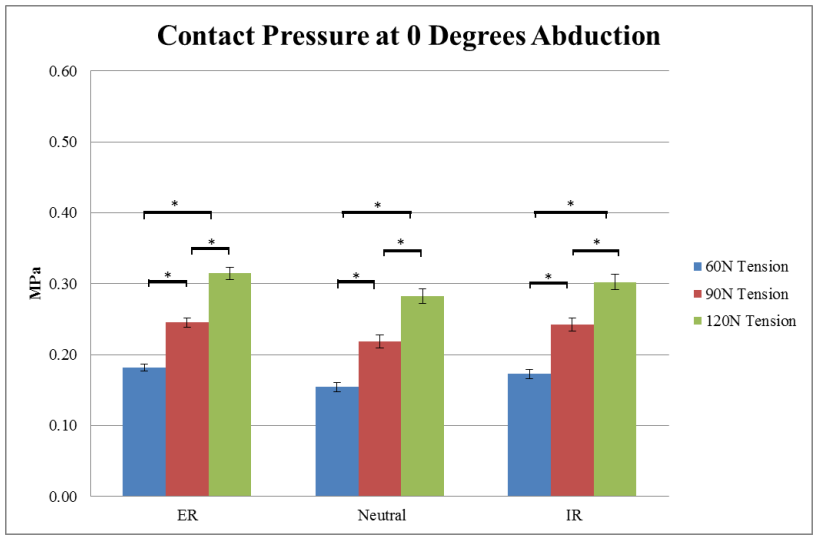

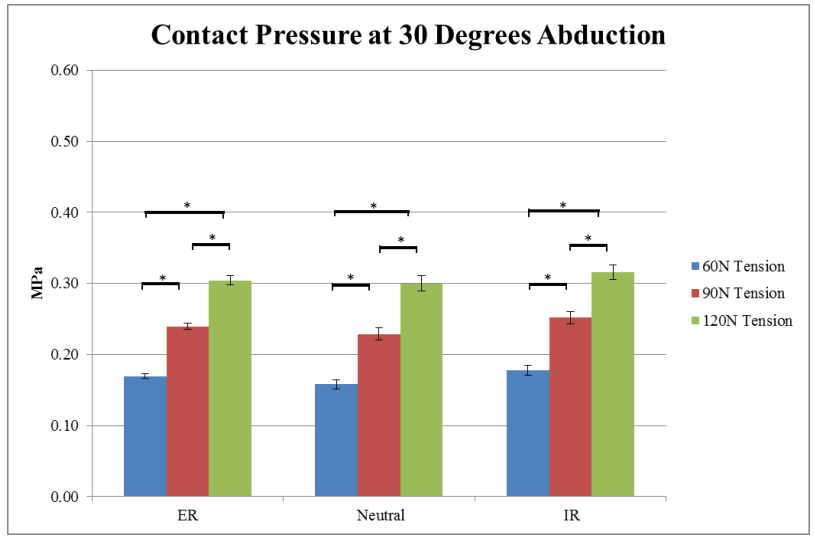

TABLE 2

Contact Area Comparisons for Bridging Suture Tension According to Various Abduction Angles and Humeral Rotations[a]

Tension, N	Contact Area, mm^2					
	Abduction 0°			Abduction 30°		
	Rotation −30°[b]	Rotation 0°	Rotation +30°	Rotation −30°[b]	Rotation 0°	Rotation +30°
60	131.5 ± 2.1	123.8 ± 2.1	128.8 ± 2.2	130.3 ± 1.8	129.9 ± 1.9	133.8 ± 2.1
90	138.9 ± 1.7	136.9 ± 1.9	133.3 ± 1.7	139.1 ± 1.8	137.2 ± 1.9	138.9 ± 1.7
120	140.2 ± 1.7	136.8 ± 1.5	140.7 ± 1.6	141.9 ± 1.8	141.1 ± 1.8	144.7 ± 1.1

[a]As tension was increased, the contact area between the repaired tendon and footprint increased, but the differences between the 90-N and 120-N groups at all positions and the 60-N and 90-N at Rotation +30°, Abduction 30° were not statistically significant.

[b]The negative angle indicates means internal rotation.

Figure 8. Footprint contact characteristics measurement is shown. As tension was increased, the contact area between the repaired cuff tendon and footprint increased, but the differences between the 90 N and 120 N groups were not statistically significant.

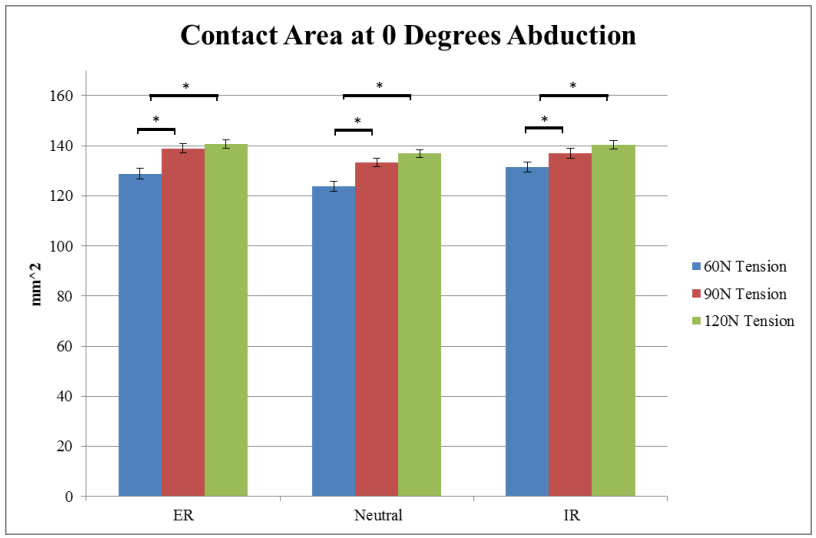

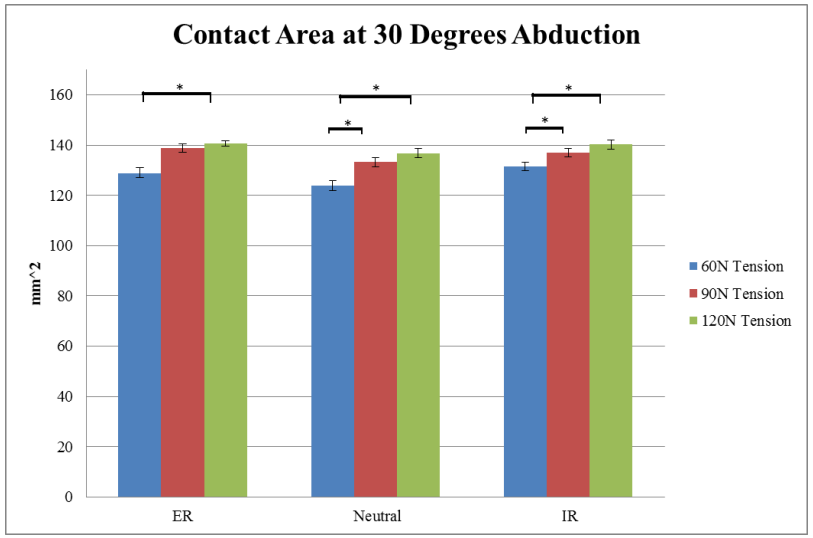

Construct Failure Test

During the cyclic-loading test, there were no statistically significant differences among the two groups (60 and 120 N of Versalok® and maximum tension of ReelX®) for the following parameters: anterior and posterior gap formation, anterior and posterior footprint strain, anterior and posterior musculotendinous junction strain, hysteresis, and initial and linear stiffness (all $P > .05$; Table 3). There was no construct failure during the cyclic-loading test.

During the load-to-failure test, there were no statistically significant differences among the 2 groups for the following parameters: initial and linear stiffness, yield load, ultimate load, absorbed energy at yield load and ultimate load, and displacement at yield load and ultimate load (all $P > .05$; Table 4).

Regarding failure mode, in the 60 N Versalok® group, there were 2 musculotendinous junction failures, 3 medial anchor failures, and 1 medial and lateral anchor failure. In the 120 N Versalok® group, there was 1 musculotendinous junction failure, 1 medial anchor failure, 1 lateral anchor failure, 1 medial and lateral anchor failure, and 2 suture failures. In the ReelX® maximum tension group, there were 2 musculotendinous junction failures, 2

medial anchor failures, and 2 medial and lateral anchor failures. We detected no direct correlation between failure mode and bridging suture tension.

TABLE 3

Gap Formation, Strain, Hysteresis, Stiffness for 60 N of Versalok® , 120 N of Versalok® , and ReelX® Maximum Tension after Cyclic Loading at Cycles 1 and 30[a]

		Cycle 1			Cycle 30		
		60 N	120 N	ReelX®	60 N	120 N	ReelX®
Gap, mm	Anterior	3.9 ± 1.7	3.2 ± 2.0	2.9 ± 1.4	5.4 ± 2.0	4.5 ± 2.4	3.5 ± 1.6
	Posterior	3.5 ± 1.2	2.5 ± 1.3	2.5 ± 0.8	4.6 ± 1.4	4.2 ± 2.1	3.7 ± 0.8
Footprint	Anterior	−5.9 ± 8.4	−10.6 ± 17.7	−9.2 ± 4.0	−5.4 ± 20.9	−4.5 ± 54.1	−3.9 ± 10.9
strain, %	Posterior	−20.7 ± 37.6	−20.7 ± 16.6	−12.4 ± 15.4	43.1 ± 54.1	20.6 ± 16.4	12.4 ± 11.2
Musculo-	Anterior	5.7 ± 19.5	11.0 ± 16.0	28.9 ± 32.1	5.6 ± 27.9	4.0 ± 21.4	32.1 ± 32.8
tendinous	Posterior	10.7 ± 7.5	14.2 ± 14.7	15.1 ± 6.5	12.3 ± 13.7	6.2 ± 7.8	19.8 ± 22.0
strain, %							

Hysteresis, N-mm	342.1 ± 36.0	305.9 ± 33.6	344.1 ± 48.7	27.9 ± 4.8	28.7 ± 5.0	33.5 ± 6.3
Initial stiffness, N/mm	24.2 ± 3.1	27.4 ± 3.7	27.9 ± 2.8	58.7 ± 12.3	55.1 ± 8.8	50.7 ± 9.7
Linear stiffness, N/mm	42.6 ± 4.1	56.7 ± 14.7	41.3 ± 3.0	117.2 ± 8.3	117.9 ± 6.8	110.2 ± 9.8

[a]There were no statistically significant differences for any variable in any group ($P > .05$).

TABLE 4

Stiffness, Yield Load, Ultimate Load, Energy Absorbed, and Gap Formation for 60 N of Versalok®, 120 N of Versalok®, and ReelX® Maximum Tension after Load-to-Failure Test[a]

	60 N	120 N	ReelX®
Initial stiffness, N/mm	58.9 ± 12.3	55.3 ± 8.9	50.8 ± 9.8
Linear stiffness, N/mm	132.9 ± 10.1	132.3 ± 9.0	125.4 ± 12.6
Yield load, N	232.4 ± 7.6	232.5 ± 5.9	235.2 ± 7.2
Ultimate load, N	553.7 ± 64.1	573.8 ± 79.2	618.4 ± 49.6
Energy absorbed at yield load, N-mm	240.8 ± 18.1	240.0 ± 10.0	268.0 ± 17.4
Energy absorbed at ultimate load, N-mm	4069.4 ± 1058.3	4825.3 ± 920.9	4741.3 ± 626.3
Gap at yield load, mm	7.6 ± 0.6	7.2 ± 0.7	7.4 ± 0.8
Gap at ultimate load, mm	15.9 ± 2.0	17.1 ± 1.4	17.0 ± 1.7

[a]There were no statistically significant differences for any variable in any group ($P > .05$).

DISCUSSION

As suture tension increased, contact force, mean pressure, and peak pressure increased accordingly. However, contact area did not increase significantly between 90 and 120 N of bridging suture tension. Although Kummer et al (16) demonstrated linear behavior between suture tension and contact area, their maximum bridging suture tension was only 80 N, and the proportionality of contact area and tension may be different with the higher tensions used in our experiment. Furthermore, there were no statistically significant differences in the construct failure test parameters in all groups. As 200 N was considered as the minimum yield load for the repaired cuff construct, all TOE constructs in the current study had enough stability to endure postoperative rehabilitation (15, 30). Therefore, our data suggest that a bridging suture tension over 90 N has no apparent benefit in this setting.

Many studies have warned about medial cuff failure with the TOE repair technique. Christoforetti et al (22) noted that bridging suture placement significantly reduced the repaired cuff tendon blood flow, even though they avoided overtensioning the bridging suture. According to Gerhardt et al (18),

strangulation with subsequent blood flow reduction at the repaired cuff area can be a possible explanation for medial cuff failure. Furthermore, Cho et al (19) has stated that undue tension at the medial row and a too-medial placement of the medial suture passage can be risk factors for medial cuff failure with the TOE repair technique. Similarly, Kummer et al (17) maintains that a large amount of bridging suture tension is not necessary for mechanical stability of the TOE construct. Based on these articles, we can assert that it is important to avoid unnecessary tension on the repaired tendon so as not to compromise blood supply. Therefore, the clinical implication of the current data is valuable for acknowledging the proper tensioning of bridging sutures

The various bridging suture tensions exerted by lateral anchor insertion did not affect the construct-failure test parameters. On the contrary, these results emphasize the importance of medial anchor fixation. Considering the shape of the TOE construct, the medial anchor is destined to receive more tension than the lateral anchor from rotator cuff muscle contracture in postoperative state. Therefore, firm fixation of the medial anchor is more important than lateral anchor fixation for the stability of the repaired cuff construct. Too much

bridging suture tension has no benefit for the stability of the TOE repair construct and poses a potential risk to compromise the vascularity of the repaired cuff tendon.

The results of the current study show that contact pressure increased proportionally as suture tension increased, similar to previous studies (13, 16). Based on the work of Andres et al (13), who demonstrated a linear relationship between bridging suture tension and contact pressure in an ovine model, we may use linear regression to estimate the bridging suture tension of other lateral suture anchors. It means that the footprint-contact characteristics data of the current study can be used as reference data for estimating bridging suture tension and contact pressure in TOE repair constructs.

In measuring the footprint-contact characteristics, the Tekscan® sensing pad, used in the current study, has several advantages. First, it allows measurement of the contact pressure in real time. Second, the measured pressure with the Tekscan® sensing pad is reversible according to exerted tension, whereas typical pressure films are not. Specifically, the colonization of pressure film is irreversible; in other words, once the pressure and area increase, the measured

pressure and area cannot decrease even after the tension is reduced. Such a characteristic is not suitable for the current study, because we wanted to be able to use manual adjustments to accurately exert different desired tensions over the course of several trials. We confirmed the reversibility of the measured parameters with the Tekscan® system in advance during the pilot studies. An additional advantage of the Tekscan® sensing pad is that it can be reused as long as its functionality and sensitivity are verified with Instron® before using again (24).

Nevertheless, the current study has a few limitations. We used a cadaveric model, which accounts only for time-zero information and cannot provide any information about repaired cuff healing. However, it is still valuable to mimic immediate postoperative clinical situations. Our data can explain exact postoperative states and serve as critical baseline information for designing clinical studies that can provide data for repaired cuff tendon healing. Lack of consideration of osteoporosis is another limitation because osteoporosis can affect the anchor pullout strength and eventually lead to construct failure. However, we note that the cadavers used in our study were relatively young

(mean age, 58.3 ± 10.9 years; range, 31–65 years), and two-thirds of the specimens were obtained from male cadavers. Furthermore, we sensed quite a firm fixation at the moment of insertion of the lateral anchor in all cases. Lastly, the VDS® marker placed on the bursal side could move differently to some extent compared with the deep tissue that is actually in contact with the footprint (15). However, because all the specimens were tested under the same conditions, this would not distort the overall trend of our results.

In conclusion, according to the current data, increasing the bridging suture tension over 90 N did not result in beneficial improvement in the contact area, although it did increase contact force and pressure. Furthermore, bridging suture tension did not significantly affect the ultimate failure loads. Therefore, considering the risks for overtensioning of bridging sutures, it might be clinically more relevant to not set the bridging suture tension over 90 N. Additionally, based on the linear correlation between bridging suture tension and contact pressure, the data presented in current study can be used as a reference for footprint characteristics. Further work includes a prospective clinical study comparing repaired cuff tendon healing at various tensions to

defrost the inherent gap between biomechanical and biologic settings and to determine the clinically optimal bridging suture tension for TOE rotator cuff repair. We envision that our current study will serve as ground work toward improving the rotator cuff healing rate and patient function and reducing many complications caused by the overtensioning of sutures.

References

1. Needell SD, Zlatkin MB, Sher JS, Murphy BJ, Uribe JW. MR imaging of the rotator cuff: peritendinous and bone abnormalities in an asymptomatic population. AJR Am J Roentgenol. 1996;166(4):863-7.

2. Yamaguchi K, Tetro AM, Blam O, Evanoff BA, Teefey SA, Middleton WD. Natural history of asymptomatic rotator cuff tears: a longitudinal analysis of asymptomatic tears detected sonographically. Journal of shoulder and elbow surgery / American Shoulder and Elbow Surgeons [et al]. 2001;10(3):199-203.

3. Oh JH, Jun BJ, McGarry MH, Lee TQ. Does a critical rotator cuff tear stage exist?: a biomechanical study of rotator cuff tear progression in human cadaver shoulders. The Journal of bone and joint surgery American volume. 2011;93(22):2100-9.

4. Fehringer EV, Sun J, VanOeveren LS, Keller BK, Matsen FA, 3rd. Full-thickness rotator cuff tear prevalence and correlation with function and co-morbidities in patients sixty-five years and older. Journal of shoulder and elbow surgery / American Shoulder and Elbow Surgeons [et al]. 2008;17(6):881-5.

5. Chung SW, Huong CB, Kim SH, Oh JH. Shoulder stiffness after rotator cuff repair: risk factors and influence on outcome. Arthroscopy : the journal of arthroscopic & related surgery : official publication of the Arthroscopy Association of North America and the International Arthroscopy Association. 2013;29(2):290-300.

6. Colvin AC, Egorova N, Harrison AK, Moskowitz A, Flatow EL. National trends in rotator cuff repair. The Journal of bone and joint surgery American volume. 2012;94(3):227-33.

7. Maman E, Harris C, White L, Tomlinson G, Shashank M, Boynton E. Outcome of nonoperative treatment of symptomatic rotator cuff tears monitored by magnetic resonance imaging. The Journal of bone and joint surgery American volume. 2009;91(8):1898-906.

8. Boileau P, Brassart N, Watkinson DJ, Carles M, Hatzidakis AM, Krishnan SG. Arthroscopic repair of full-thickness tears of the

supraspinatus: does the tendon really heal? The Journal of bone and joint surgery American volume. 2005;87(6):1229-40.

9. Oh JH, Kim SH, Kang JY, Oh CH, Gong HS. Effect of age on functional and structural outcome after rotator cuff repair. Am J Sports Med. 2010;38(4):672-8.

10. Chung SW, Kim JY, Kim MH, Kim SH, Oh JH. Arthroscopic repair of massive rotator cuff tears: outcome and analysis of factors associated with healing failure or poor postoperative function. Am J Sports Med. 2013;41(7):1674-83.

11. Chung SW, Oh JH, Gong HS, Kim JY, Kim SH. Factors affecting rotator cuff healing after arthroscopic repair: osteoporosis as one of the independent risk factors. Am J Sports Med. 2011;39(10):2099-107.

12. Park MC, ElAttrache NS, Tibone JE, Ahmad CS, Jun BJ, Lee TQ. Part I: Footprint contact characteristics for a transosseous-equivalent rotator cuff repair technique compared with a double-row repair technique. Journal of shoulder and elbow surgery / American Shoulder and Elbow Surgeons [et al]. 2007;16(4):461-8.

13. Andres BM, Lam PH, Murrell GA. Tension, abduction, and surgical technique affect footprint compression after rotator cuff repair in an ovine model. Journal of shoulder and elbow surgery / American Shoulder and Elbow Surgeons [et al]. 2010;19(7):1018-27.

14. Ahmad CS, Stewart AM, Izquierdo R, Bigliani LU. Tendon-bone interface motion in transosseous suture and suture anchor rotator cuff repair techniques. Am J Sports Med. 2005;33(11):1667-71.

15. Park MC, Tibone JE, ElAttrache NS, Ahmad CS, Jun BJ, Lee TQ. Part II: Biomechanical assessment for a footprint-restoring transosseous-equivalent rotator cuff repair technique compared with a double-row repair technique. Journal of shoulder and elbow surgery / American Shoulder and Elbow Surgeons [et al]. 2007;16(4):469-76.

16. Kummer FJ. Effects of suture tension on the footprint of rotator cuff repairs--technical note. Bull NYU Hosp Jt Dis. 2012;70(4):259-61.

17. Kummer F, Hergan DJ, Thut DC, Pahk B, Jazrawi LM. Suture loosening and its effect on tendon fixation in knotless double-row rotator cuff repairs. Arthroscopy : the journal of arthroscopic & related surgery :

official publication of the Arthroscopy Association of North America and the International Arthroscopy Association. 2011;27(11):1478-84.

18. Gerhardt C, Hug K, Pauly S, Marnitz T, Scheibel M. Arthroscopic single-row modified mason-allen repair versus double-row suture bridge reconstruction for supraspinatus tendon tears: a matched-pair analysis. Am J Sports Med. 2012;40(12):2777-85.

19. Cho NS, Yi JW, Lee BG, Rhee YG. Retear patterns after arthroscopic rotator cuff repair: single-row versus suture bridge technique. Am J Sports Med. 2010;38(4):664-71.

20. Trantalis JN, Boorman RS, Pletsch K, Lo IK. Medial rotator cuff failure after arthroscopic double-row rotator cuff repair. Arthroscopy : the journal of arthroscopic & related surgery : official publication of the Arthroscopy Association of North America and the International Arthroscopy Association. 2008;24(6):727-31.

21. Yamakado K, Katsuo S, Mizuno K, Arakawa H, Hayashi S. Medial-row failure after arthroscopic double-row rotator cuff repair. Arthroscopy : the journal of arthroscopic & related surgery : official publication of the Arthroscopy Association of North America and the International Arthroscopy Association. 2010;26(3):430-5.

22. Christoforetti JJ, Krupp RJ, Singleton SB, Kissenberth MJ, Cook C, Hawkins RJ. Arthroscopic suture bridge transosseus equivalent fixation of rotator cuff tendon preserves intratendinous blood flow at the time of initial fixation. Journal of shoulder and elbow surgery / American Shoulder and Elbow Surgeons [et al]. 2012;21(4):523-30.

23. Domb BG, Glousman RE, Brooks A, Hansen M, Lee TQ, ElAttrache NS. High-tension double-row footprint repair compared with reduced-tension single-row repair for massive rotator cuff tears. The Journal of bone and joint surgery American volume. 2008;90 Suppl 4:35-9.

24. Park MC, Pirolo JM, Park CJ, Tibone JE, McGarry MH, Lee TQ. The effect of abduction and rotation on footprint contact for single-row, double-row, and modified double-row rotator cuff repair techniques. Am J Sports Med. 2009;37(8):1599-608.

25. Park MC, Idjadi JA, Elattrache NS, Tibone JE, McGarry MH, Lee TQ. The effect of dynamic external rotation comparing 2 footprint-restoring rotator cuff repair techniques. Am J Sports Med. 2008;36(5):893-900.
26. Reilly P, Bull AM, Amis AA, Wallace AL, Richards A, Hill AM, et al. Passive tension and gap formation of rotator cuff repairs. Journal of shoulder and elbow surgery / American Shoulder and Elbow Surgeons [et al]. 2004;13(6):664-7.
27. Barber FA, Hapa O, Bynum JA. Comparative testing by cyclic loading of rotator cuff suture anchors containing multiple high-strength sutures. Arthroscopy : the journal of arthroscopic & related surgery : official publication of the Arthroscopy Association of North America and the International Arthroscopy Association. 2010;26(9 Suppl):S134-41.
28. Barber FA, Coons DA, Ruiz-Suarez M. Cyclic load testing of biodegradable suture anchors containing 2 high-strength sutures. Arthroscopy : the journal of arthroscopic & related surgery : official publication of the Arthroscopy Association of North America and the International Arthroscopy Association. 2007;23(4):355-60.
29. Park MC, Bui C, Park CJ, Oh JH, Lee TQ. Rotator cuff tendon repair morphology comparing 2 single-anchor repair techniques. Arthroscopy : the journal of arthroscopic & related surgery : official publication of the Arthroscopy Association of North America and the International Arthroscopy Association. 2013;29(7):1149-56.
30. Burkhart SS. A stepwise approach to arthroscopic rotator cuff repair based on biomechanical principles. Arthroscopy : the journal of arthroscopic & related surgery : official publication of the Arthroscopy Association of North America and the International Arthroscopy Association. 2000;16(1):82-90.

초록

관절경적 회전근 개 교량형 봉합술시 봉합사에 가해지는 적절한 장력에 대한 사체 생 역학 연구

박 지 순

서울대학교 대학원

의학과 정형외과학 전공

서론: 관절경적 회전근 개 봉합시 사용되는 교량형 봉합술식 (TOE : trans-osseous equivalent) 은 봉합된 회전근 개 건과 상완골 부착부위 사이의 접촉 면적을 최대화하며 보다 높은 압력으로 부착되게 하여 사이의 들뜸 (gap formation) 을 최소화하는 것으로 보고되고 있으며, 봉합된 구조물이 보다 높은 최대 하중 (ultimate load)에 견딜 수 있는 것으로 알려져 있다. 그러나, 회전근 개 교량형 봉합 이후 발생하는 내측부 재파열 (medial cuff failure) 의

원인이 지나치게 증가시킨 교량 봉합사의 장력 때문이라는 주장이 제기 되고 있다. 이에 저자들은 사체 생 역학 연구를 통해, 회전근개 교량형 봉합시 교량 봉합사에 걸리는 장력과 건-부착 부위 압력 및 접촉 면적의 상관 관계에 대한 정보를 수집하고, 봉합된 구조물의 안정성에 대한 자료를 종합하여, 교량형 봉합술식에서의 적절한 교량 봉합사의 장력을 확인해 보고자 하였다.

방법: 총 18 구의 사체 어깨를 준비하였으며, 이를 무작위로 세 개의 군 (A, B, R) 으로 나누었다. 모든 사체 어깨는 동일한 내측 나사못 (Healix®, Depuy Mitek, Raynham, MA) 을 사용하여 교량형 봉합술식으로 봉합 하였으며, 건과 부착 부위 사이에는 Tekscan® 압력 측정장치를 부착하였다. 이 중 9 개의 사체 어깨를 교량 봉합사의 장력과 건-부착 부위 압력 및 접촉 면적에 대한 상관관계 분석에 사용하였다. 예비 연구를 통해 분석에 사용될 교량 봉합사의 장력은 60, 90, 120N 으로 정하였으며, 견관절 외전 각도 0, 30° 및 견관절 회전 각도 −30, 0, 30° 의 자세에서 각각 분석을 진행하였다. 건 부착 부위 압력 및 접촉 면적에 대한 분석 종료 후,

모든 18 개의 사체 어깨를 세 군으로 나누어 봉합된 구조물의 안정성에 대한 실험을 진행하였다. A, B 군은 Versalok® (Depuy Mitek, Raynham, MA) 외측 나사못을 삽입하였으며 각각 60, 120N 의 장력을 가하였고, R 군은 ReelX® (Stryker Endoscopy, San Jose, CA) 외측 나사못을 최대 장력으로 삽입하였다. 이후 봉합된 구조물에 대한 항복 하중 (yield load), 최대 하중 (ultimate load), 이력 (hysteresis), 강성 (stiffness), 파괴 양상(mode of failure) 등을 확인하였다.

결과: 교량 봉합사의 장력을 증가 시킬수록, 건-부착부위 사이의 접촉력 (contact force), 접촉 압력 (contact pressure) 및 최대 접촉 압력 (peak contact pressure) 은 실험에 사용된 모든 견관절 자세에서 통계적으로 의미 있는 증가를 보였다(모두 $p < 0.05$). 그러나, 접촉 면적 (contact area) 의 경우 교량 봉합사의 장력을 60N 에서 90N 으로 증가시키는 경우에는 통계적으로 의미 있는 증가를 보였으나, 90N 에서 120N 으로 증가시키는 경우에는 모든 견관절 자세에서 의미 있는 증가를 보이지 않았다. 봉합된 구조물의

안정성에 대한 실험에서는 교량 봉합사의 장력의 차이나 외측 나사못의 종류에 따른 의미 있는 차이는 관찰 되지 않았다. (모두 $p > 0.05$)

결론: 상기의 실험 결과에 따르면, 90N 이상의 교량 봉합사 장력은 접촉력이나 접촉 압력의 경우 의미 있는 증가를 가져오나, 접촉 면적에 대해서는 의미 있는 증가를 보여주지 않았다. 더구나, 교량 봉합사의 장력은 봉합된 구조물의 안정성에 큰 영향을 끼치지 않은 것으로 나타났다. 교량 봉합사의 장력을 지나치게 증가시킬 경우 발생할 수 있는 내측부 재파열의 위험성을 고려할 때, 교량형 봉합술식에서의 교량 봉합사의 장력은 90N 이상으로 증가시키지 않는 것이 임상적으로 타당할 것으로 생각된다.

주요 단어 : 회전근 개 봉합술, 교량형 봉합술식, 교량 봉합사 장력

학 번: 2012-23615